British Journal of Pharmacology

British Journal of Pharmacology (2018) **175** 2470–2482 2470

RESEARCH PAPER

Selective late sodium current inhibitor GS-458967 suppresses Torsades de Pointes by mostly affecting perpetuation but not initiation of the arrhythmia

Correspondence Alexandre Bossu, PhD, Department of Medical Physiology, Division Heart & Lungs, University Medical Center Utrecht, Yalelaan 50, Utrecht 3584 CM, The Netherlands. E-mail: a.bossu@umcutrecht.nl

Received 29 August 2017; **Revised** 27 February 2018; **Accepted** 2 March 2018

Alexandre Bossu[1], Marien J C Houtman[1], Veronique M F Meijborg[2], Rosanne Varkevisser[1], Henriette D M Beekman[1], Albert Dunnink[1], Jacques M T deBakker[1,2], Nevena Mollova[3], Sridharan Rajamani[4], Luiz Belardinelli[5], Marcel A G van derHeyden[1] and Marc A Vos[1]

[1]Department of Medical Physiology, Division Heart & Lungs, University Medical Center Utrecht, Utrecht, The Netherlands, [2]Department of Experimental Cardiology, Amsterdam Medical Center, Amsterdam, The Netherlands, [3]Gilead Sciences, Inc., Foster City, CA, USA, [4]Amgen, San Francisco, CA, USA, and [5]InCarda Therapeutics, Newark, CA, USA

BACKGROUND AND PURPOSE

Enhanced late sodium current (late I_{Na}) in heart failure and long QT syndrome type 3 is proarrhythmic. This study investigated the antiarrhythmic effect and mode of action of the selective and potent late I_{Na} inhibitor GS-458967 (GS967) against Torsades de Pointes arrhythmias (TdP) in the chronic atrioventricular block (CAVB) dog.

EXPERIMENTAL APPROACH

Electrophysiological and antiarrhythmic effects of GS967 were evaluated in isolated canine ventricular cardiomyocytes and CAVB dogs with dofetilide-induced early afterdepolarizations (EADs) and TdP, respectively. Mapping of intramural cardiac electrical activity *in vivo* was conducted to study effects of GS967 on spatial dispersion of repolarization.

KEY RESULTS

GS967 (IC_{50}~200nM) significantly shortened repolarization in canine ventricular cardiomyocytes and sinus rhythm (SR) dogs, in a concentration and dose-dependent manner. *In vitro*, despite addition of 1 μM GS967, dofetilide-induced EADs remained present in 42% and 35% of cardiomyocytes from SR and CAVB dogs, respectively. Nonetheless, GS967 (787±265nM) completely abolished dofetilide-induced TdP in CAVB dogs (10/14 after dofetilide to 0/14 dogs after GS967), while single ectopic beats (sEB) persisted in 9 animals. *In vivo* mapping experiments showed that GS967 significantly reduced spatial dispersion of repolarization: cubic dispersion was significantly decreased from 237±54ms after dofetilide to 123±34ms after GS967.

CONCLUSION AND IMPLICATIONS

GS967 terminated all dofetilide-induced TdP without completely suppressing EADs and sEB *in vitro* and *in vivo*, respectively. The antiarrhythmic mode of action of GS967, through the reduction of spatial dispersion of repolarization, seems to predominantly impede the perpetuation of arrhythmic events into TdP rather than their initiating trigger.

Abbreviations

APD, action potential duration; AS, arrhythmia score; CAVB, chronic atrioventricular block; EAD, early afterdepolarization; EB, ectopic beat; GS-458967, (GS967) (6-(4-(trifluoromethoxy)phenyl)-3-(trifluoromethyl)(1,2,4)triazolo(4,3-a)pyridine; I_{Kr}, rapid component of the delayed rectifier potassium outward current; I_{Ks}, slow component of the delayed rectifier potassium outward current; late I_{Na}, late sodium current; LV, left ventricle; MAPD, monophasic action potential duration; RV, right ventricle; SR, sinus rhythm; STV, short-term variability; TdP, Torsades de Pointes; TTX, tetrodotoxin

DOI:10.1111/bph.14217

Introduction

In cells of ventricular myocardium, the activation of the sodium channel isoform **$Na_V1.5$** results in a prominent transient inward sodium current (peak I_{Na}) responsible for the upstroke of the cardiac action potential. While most of these channels rapidly inactivate, a small fraction of them may remain open or reactivate giving rise to a sustained depolarizing sodium current (late I_{Na}) throughout the plateau phase of the action potential (Zaza *et al.*, 2008). The late I_{Na}, despite its small amplitude (Saint, 2008), interferes with the repolarization process by countering the effect of the rapid and slow components of the delayed rectifier outward potassium currents (**I_{Kr}** and **I_{Ks}**, respectively). Hence, in conditions of increased late I_{Na}, as observed in heart failure (Maltsev and Undrovinas, 2006) or in the congenital long QT syndrome type 3 (Bezzina *et al.*, 2015), this current is known to be pro-arrhythmic (Antzelevitch *et al.*, 2014; Belardinelli *et al.*, 2015). Late I_{Na} lengthens action potential duration (APD), reduces repolarization reserve and causes sodium-dependent calcium overload in cardiomyocytes (Belardinelli *et al.*, 2013; Shryock *et al.*, 2013).

Over the years, several I_{Na} inhibitors have been developed and used as antiarrhythmic drugs, such as **flecainide** or more recently **ranolazine**. While preferably blocking the late component of I_{Na}, flecainide and ranolazine respectively inhibit in parallel peak I_{Na} and I_{Kr} (Antzelevitch *et al.*, 2004; Schram *et al.*, 2004; Belardinelli *et al.*, 2013), which can lead to adverse effects including slowing of conduction (Tamargo *et al.*, 2012) or QT prolongation (Chaitman *et al.*, 2004). Despite lengthening repolarization, ranolazine is not pro-arrhythmic and even exhibited antiarrhythmic properties against ventricular arrhythmias in a number of studies (Antoons *et al.*, 2010; Pulford and Kluger, 2016) demonstrating the potential of late I_{Na} inhibition to prevent ventricular arrhythmias such as in the chronic atrioventricular block (CAVB) dog model (Antoons *et al.*, 2010). This well-characterized animal model features a compensated biventricular hypertrophy and an enhanced susceptibility to drug-induced Torsades de Pointes (TdP) arrhythmias. Incidence of these arrhythmic episodes is strongly associated with electrical remodelling including the down-regulation of I_{Kr} and I_{Ks} as well as a disturbed calcium handling (Oros *et al.*, 2008). In the CAVB dog model, ranolazine moderately prevented and suppressed TdP episodes (Antoons *et al.*, 2010). However, within the range of clinical concentrations, ranolazine interacts with other ion currents, such as I_{Kr} (Antzelevitch *et al.*, 2004; Schram *et al.*, 2004), **I_{CaL}** (Allen and Chapman, 1996; Antzelevitch *et al.*, 2004), or the **ryanodine receptor** (Parikh *et al.*, 2012), which makes the interpretation of late I_{Na} block *per se* to prevent ventricular arrhythmias difficult.

The selective and potent late I_{Na} inhibitor GS-458967 (GS967) has minimal effects on other cardiac ion currents (Belardinelli *et al.*, 2013), cardiac contractility (Fernandes *et al.*, 2014) and conduction velocity. Antiarrhythmic properties of GS967 were demonstrated *in vitro* (Belardinelli *et al.*, 2013; Sicouri *et al.*, 2013) as well as in a number of *in vivo* ventricular (Belardinelli *et al.*, 2013; Bonatti *et al.*, 2014; Pezhouman *et al.*, 2014; Alves Bento *et al.*, 2015) and atrial (Burashnikov *et al.*, 2015; Carneiro *et al.*, 2015) arrhythmia models but not in the CAVB dog. The use of this canine model would provide additional information relevant for clinical applications due to the comparable cardiac electrophysiology between dogs and humans. In addition, this sensitive model reflects the pro-arrhythmic vulnerability of patients at compensated and early stage of heart failure (Sipido *et al.*, 2002; Allen *et al.*, 2012).

The goal of the present study was to evaluate and elucidate the antiarrhythmic efficacy and mode of action of the selective late I_{Na} inhibitor GS967 in the CAVB dog. This was done by investigating the suppression of early afterdepolarizations (EADs) of isolated canine ventricular cardiomyocytes *in vitro* and the termination of TdP in CAVB dogs *in vivo* in relation to the effect on spatial dispersion of repolarization.

Methods

General

Animal care, management and experiments were performed in accordance with guidelines from the Directive 2010/63/EU of the European Parliament, the Council of 22 September 2010 on the protection of animals used for scientific purposes and the Dutch law on animal experimentation. Protocols were approved by the Committee for Experiments on Animals of Utrecht University (2013.II.08.088). Animal studies are reported in compliance with the ARRIVE guidelines (Kilkenny *et al.*, 2010; McGrath and Lilley, 2015). The current study has no implications for replacement, reduction or refinement.

A total of 18 adult mongrel dogs (Marshall, NY, USA; 5 male, 25 ± 3 kg, 16 ± 5 months old) were included in the *in vivo* protocol. Dogs, housed in pairs in conventional kennels (~8 m^2) including wooden bedding, had free access to water *ad libitum* and received food pellets twice a day. Each cage was supplied with playing tools, and animals were allowed to play in a group within an outdoor pen (~50 m^2) during the day. The well-being and health of the animals were monitored daily, and they were weighed once a week and prior to experiments.

After premedication, which included atropine (0.5 mg i.m.; Pharmachemie BV, Haarlem, The Netherlands), methadone (10 mg i.m., COMFORTAN®; Eurovet Animal Health BV, Bladel, The Netherlands), meloxicam (2 $mg \cdot kg^{-1}$ s.c., METACAM®; Boehringer-Ingelheim Vetmedica BV, Ingelheim am Rhein, Germany) and acepromazine (10 mg i.m., VETRANQUIL®; Alfasan BV, Woerden, The Netherlands), all experiments were performed under general anaesthesia induced by pentobarbital (25 $mg \cdot kg^{-1}$ i.v.) and maintained by isoflurane (1.5%; Abbot Laboratories Ltd, Maidenhead, UK; in an O_2/N_2O mixture; 2:1). Perioperative care included the administration of an antibiotic (ampicillin 1000 mg i.v. before and i.m. after experiment, AMPI-DRY®; DopharmaBV, Raamsdonksveer, The Netherlands) and analgesia (buprenorphin 0.3 mg i.m. after experiment, TEMGESIC®; Indivior UK Ltd, Slough, UK). Surface ECG was continuously recorded along with endocardial left and right ventricular monophasic action potentials [left ventricle (LV) and right ventricle (RV) monophasic action potential (MAP), respectively; Hugo Sachs,

Germany] by EPTracer software (Cardiotek, Maastricht, The Netherlands). After the sinus rhythm (SR) protocol was completed, a screw-in lead was advanced to the RV apex *via* the jugular vein and connected to an internal pacemaker (different models; Medtronic, Maastricht, The Netherlands). The atrioventricular (AV) node was then ablated using radiofrequency. CAVB experiments were performed after at least 3 weeks under idioventricular rhythm, once electrical remodelling is completed (Oros *et al.*, 2008).

ECG intervals were measured offline with EPTracer and averaged over five consecutive beats. QT interval was corrected for heart rate (QTc) using the van de Water formula [$QTc = QT - 0.087 \times (RR - 1000)$].

LV and RV MAP duration (MAPD) at 80% repolarization and their associated short-term variability (STV, calculated as $STV = \Sigma \mid D_{n+1} + D_n - 2D_{mean} \mid /[30 \times \sqrt{2}]$ as previously described; Thomsen *et al.*, 2004) values were obtained from 30 consecutive beats using custom made (Dr P. Oosterhoff) software (AutoMAPD, Matlab; MathWorks, Natick, MA, USA). The interventricular dispersion of repolarization, ΔMAPD, was determined as the difference LV MAPD − RV MAPD.

Sinus rhythm protocol

GS967 was sequentially administered at 0.03 and 0.1 mg·kg^{-1} over 5 min (30 min interval between doses) to 10 dogs in SR. Electrophysiological parameters were recorded along with LV pressure *via* a sensor catheter (CD Leycom Inc., Zoetermeer, The Netherlands). Blood samples were collected every 5 min for determination of GS967 plasma levels by HPLC (Gilead Sciences, Inc., Foster City, CA, USA).

Antiarrhythmic protocols in chronic atrioventricular block dogs

Suppression protocol. Nine CAVB dogs were acutely paced during the experiment *via* their internal pacemaker (60 beats·min^{-1}, n = 8; 65 beats·min^{-1}, n = 1). After a 10 min baseline period, **dofetilide** (25 μg·kg^{-1}) was applied for 5 min to induce TdP. GS967 (0.1 mg·kg^{-1} per 5 min) was administered after incidence of TdP 10 min after start of dofetilide infusion. A TdP episode was defined as a polymorphic ventricular tachycardia characterized by at least five consecutive ectopic beats (EBs) with a twisting shape of the QRS complex around the isoelectric line. Defibrillation was applied when an arrhythmia episode lasted more than 10 s. Ventricular arrhythmias were monitored for 10 min during baseline, dofetilide (from start of infusion to start of GS967) and GS967 periods (after end of infusion) using two different approaches. First, the incidence of arrhythmias (≥3 episodes) was determined for single ectopic beat (sEB), multiple ectopic beat (mEB) and TdP. Second, an arrhythmia score (AS) was calculated over the corresponding period as the average of the three most severe arrhythmic events: normal beat 1 point, sEB 2 points, mEB 3 to 5 points, run of TdP 6 to 49 points and number of successive defibrillations to restore normal paced heart rhythm (1, 2 or ≥3; 50, 75 or 100 points, respectively).

Electrophysiological parameters derived from surface ECG and MAP recordings were measured at baseline, after dofetilide (first EB/TdP or 5 min) and at the end of GS967 infusion.

Mapping experiment. In five additional CAVB paced dogs (60 beats·min^{-1}, n = 4; 70 beats·min^{-1}, n = 1) and using the same experimental setting, the antiarrhythmic mechanism of GS967 was further characterized in a detailed electrical mapping experiment, which consisted of the insertion of a total of 56 needle electrodes at six different levels of the heart (from base to apex, Figure 1) as previously described by our group (Dunnink *et al.*, 2017). The needles had four electrode terminals (4 mm interelectrode interval) to record intramural unipolar electrograms (ActiveTwo system; Biosemi, Amsterdam, The Netherlands). In addition to the ECG intervals, repolarization time (RT) of all recorded electrograms was determined at baseline, before dofetilide-induced first EB and TdP (or 5 min after start of dofetilide if TdP not inducible) and after GS967 administration using a custom-made data analysis programme written in Matlab (version R2014a; MathWorks). For each of these time points, the local spatial dispersion of repolarization was calculated from the LV and septal wall between adjacent electrodes according to transmural, vertical, horizontal and cubic orientations (Figure 1).

Randomization and analysis

Animals were not randomized in the present study as each dog served as its own control (baseline period) at either of the conditions tested (SR and CAVB). The remodelling processes occurring after creation of AV block, at the structural, mechanical and electrical levels, have been well described in this animal model (Oros *et al.*, 2008). The inducibility of TdP arrhythmias upon dofetilide administration persist for more than 20 min (Oros *et al.*, 2008), which allows the testing of (pharmacological) antiarrhythmic interventions (Bossu *et al.*, 2017).

Animal experiments and data analyses were not performed under blind conditions. All 10 SR dogs received GS967 consecutively at 0.03 and 0.1 mg·kg^{-1} over 5 min. In addition, dofetilide followed by GS967 were both administered to all 14 CAVB dogs. The induction of reproducible TdP episodes by dofetilide can be easily visualized on the surface ECG during the experiment. Likewise, the successful antiarrhythmic efficacy of GS967, ability to suppress TdP episodes, was also evident during the experiments.

Cellular experiments

At the end of the last *in vivo* experiment, a right thoracotomy was performed, and the heart was quickly excised. Cellular experiments were performed on ventricular cardiomyocytes isolated from 15 CAVB dogs (including six animals from the *in vivo* protocol) and from 11 additional age-matched Beagle dogs in SR (provided by WIL Research, 's-Hertogenbosch, The Netherlands) using the whole-cell patch-clamp technique. The isolation procedure was as described previously (Nalos *et al.*, 2012). Canine ventricular cardiomyocytes were enzymatically isolated from the heart of 11 SR and 15 CAVB dogs. After a right thoracotomy, hearts were quickly excised and washed with PBS solution and flushed with ice-cold Ca^{2+} free standard buffer solution (in mM: NaCl 130, KCl 5.4, KH_2PO_4 1.2, $MgSO_4$ 1.2, HEPES 6 and glucose 20, pH 7.2 corrected with NaOH). The left circumflex coronary artery (for LV cardiomyocytes) and right coronary artery (for RV cardiomyocytes) were cannulated and perfused by gravity

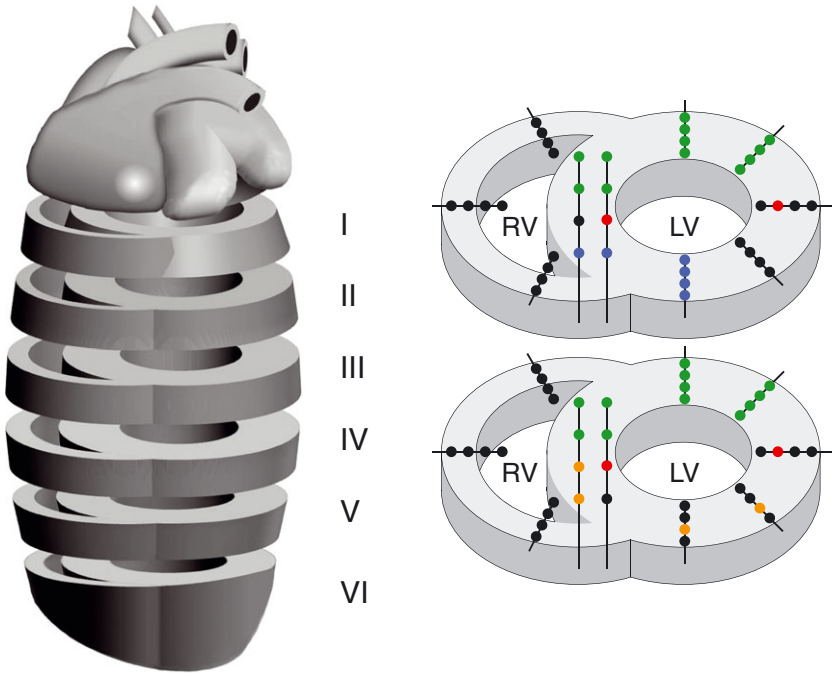

Figure 1

Overview of needle location and calculation of spatial dispersion of repolarization in the detailed mapping experiments (adapted from Dunnink *et al.*, 2017 with permission). A total of 56 needles were inserted over six different levels of the heart, from base to apex (I to VI): in the LV, 30 needles were divided into five columns (posterior, postero-lateral, lateral, antero-lateral and anterior); in the RV, 18 needles were divided into three columns (posterior, lateral and anterior) and 8 needles in the septal wall (left and right sides, levels II to V, in three dogs). Dispersion of repolarization in the LV (n = 5 dogs) and in the septal wall (n = 3 dogs) was determined within adjacent electrodes of one needle (transmural dispersion, blue electrodes), one column (vertical dispersion, red electrodes), one level (horizontal dispersion, orange electrodes) and within a square of four needles (cubic dispersion, green electrodes). Maximal differences were retrieved from each orientation.

on a Langendorff set-up with solutions warmed at 37°C: (i) 10 min of Ca^{2+} free standard buffer solution; (ii) 25–35 min of enzymatic solution consisting of 400 mL Ca^{2+} free standard buffer solution with 420 mg collagenase A (Roche, Indianapolis, IN, USA), 32 mg protease (Sigma-Aldrich, Zwijndrecht, The Netherlands) and 400 μL trypsin 2.5%; and (iii) 10 min of 0.2 mM Ca^{2+} standard buffer solution (Ca^{2+} free standard buffer solution with 0.2 mM $CaCl_2$). LV and RV midmyocardial tissue was then harvested, and the cell suspensions were filtered. Isolated cardiomyocytes were kept at room temperature in 0.2 mM Ca^{2+} standard buffer solution and used for patch-clamp experiments the same day. Patch-clamp data were acquired and analysed using the pCLAMP 10 software (Molecular Devices, Sunnyvale, CA, USA).

Late sodium current density and inhibition by GS967. In LV and RV cardiomyocytes from SR and CAVB dogs, I_{Na} was elicited by applying 500 ms pulses to −20 mV (0.25 Hz) from a holding potential of −100 mV. Late sodium current (late I_{Na}) was quantified as the **tetrodotoxin** (TTX)-sensitive current between 200 and 220 ms after the pulse onset and normalized to cell capacitance. Patch pipettes (resistance 1.5–2.5 MΩ) were filled with the internal solution (in mM) NaCl 5, CsCl 133, MgATP 2, tetraethylammonium chloride 20, EGTA 10 and HEPES 5, pH 7.3 with CsOH. Cells were continuously superfused with a 22 ± 1°C bath solution containing (in mM) NaCl 140, CsCl 5, $CaCl_2$ 1.8, $MgCl_2$ 2, glucose 5, HEPES 5 and nifedipine 0.002, pH 7.3 with CsOH. Late I_{Na} inhibition by GS967 (30, 100, 300 and 1000 nM) was normalized against total late I_{Na} in each cardiomyocyte.

Effect of GS967 on repolarization and ability to suppress early afterdepolarizations. Action potentials were elicited at 0.5 Hz. External solution (37 ± 1°C) consisted of (in mM) NaCl 137, KCl 5.4, $MgCl_2$ 0.5, $CaCl_2$ 1.8, HEPES 11.8 and glucose 10 (pH 7.4) and internal solution of KCl 130, NaCl 10, HEPES 10, MgATP 5 and $MgCl_2$ 0.5 (pH 7.2). GS967 (100, 300 or 1000 nM) was added to the superfusate after a control period of 3 min to investigate the effect of selective late I_{Na} inhibition on repolarization. APD at 90% of repolarization and the associated STV after GS967 were normalized against their respective baseline condition to determine any concentration-dependent effect.

Additionally, GS967 (same concentrations) was superfused after dofetilide-induced EADs to determine the potential *in vitro* antiarrhythmic properties of the compound.

Materials

GS967 (Gilead Science Inc., Foster City, CA, USA) was stored as 10 mM stock solution in DMSO. Solutions for *in vivo* and *in vitro* purposes were freshly prepared prior to experiments.

Dofetilide, supplied by Procter & Gamble Pharmaceuticals (Cincinnati, OH, USA), was dissolved in 100 μL HCl 0.1 M and diluted into saline solution to obtain the desired concentration. Stock solution of dofetilide 10 mM in DMSO was diluted to Tyrode solution for patch-clamp experiments. Aqueous stock solution of TTX 10 mM was similarly added to external solutions for I_{Na} recordings.

Statistical analysis

The data and statistical analysis comply with the recommendations on experimental design and analysis in pharmacology (Curtis *et al.*, 2015). Data are expressed as mean ± SD. Comparisons of serial data were performed with a paired *t*-test or one-way repeated measures ANOVA using a *post hoc* Bonferroni correction (parametric and non-parametric test). The McNemar test was used for the analysis of arrhythmias incidence. All statistical analyses were performed with Prism (Version 6.0c; GraphPad Software, La Jolla, CA, USA). Differences were considered significant when $P < 0.05$.

Nomenclature of targets and ligands

Key protein targets and ligands in this article are hyperlinked to corresponding entries in http://www.guidetopharmacology.org, the common portal for data from the IUPHAR/BPS Guide to PHARMACOLOGY (Harding *et al.*, 2018), and are permanently archived in the Concise Guide to PHARMACOLOGY 2015/16 (Alexander *et al.*, 2017).

Results

Late sodium current inhibition shortens repolarization in vitro and in vivo

Late sodium current in ventricular cardiomyocytes and inhibition by GS967. In ventricular cardiomyocytes isolated from unremodelled dogs in SR, the late I_{Na} density was more prominent in the LV than in the RV (0.30 ± 0.10 vs. 0.21 ± 0.10 pA·pF^{-1}, $P < 0.05$; Figure 2A). In cardiomyocytes from CAVB dogs, after electrical remodelling, the late I_{Na} density was lower in both ventricles but only significantly in the LV (from 0.30 ± 0.10 pA·pF^{-1} in SR to 0.18 ± 0.05 pA·pF^{-1} in CAVB, $P < 0.05$; Figure 2A).

GS967 inhibited the late I_{Na} concentration dependently (Figure 2B) in ventricular cardiomyocytes isolated from SR and CAVB dogs (Figure 2C). In CAVB cardiomyocytes, GS967 at 30, 100, 300 and 1000 nM reduced late I_{Na} magnitude in a concentration-dependent manner (Figure 2C).

GS967 reduces action potential duration in ventricular cardiomyocytes. To determine the effect of selective late I_{Na} inhibition on APD, GS967 was tested at 100, 300 and 1000 nM in ventricular cardiomyocytes from CAVB dogs. As

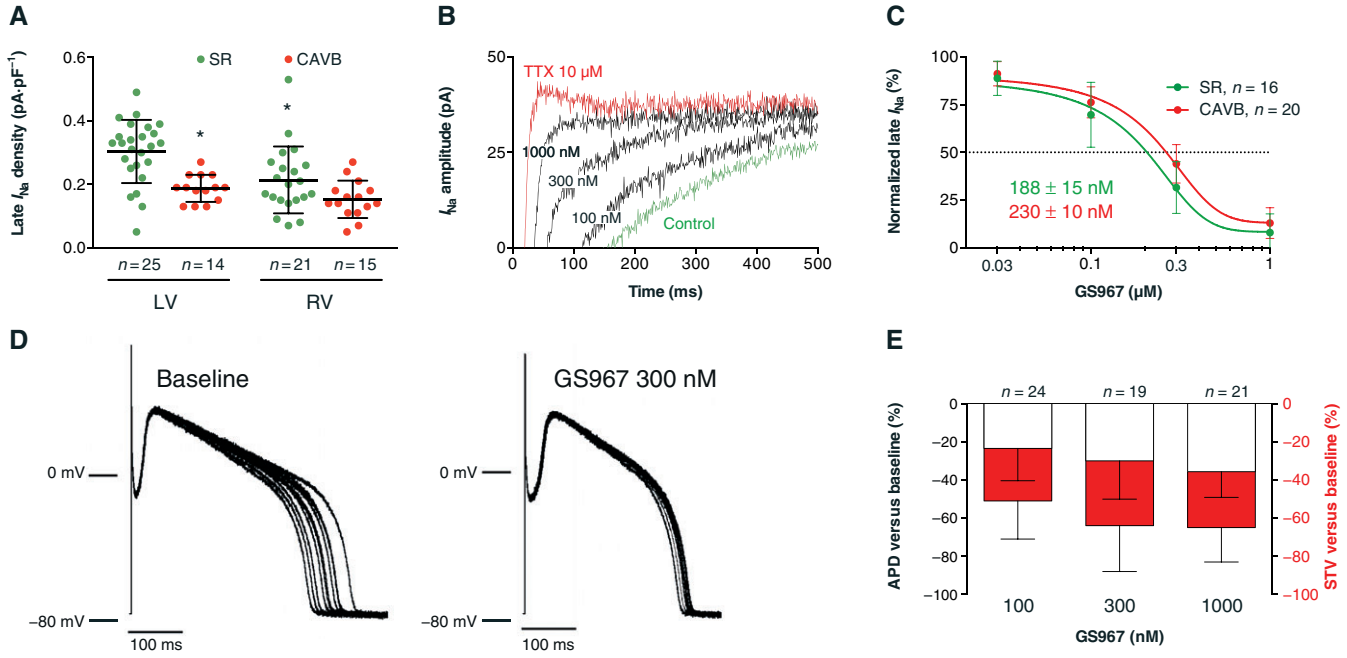

Figure 2

Late sodium current is lower in ventricular cardiomyocytes of CAVB dog (A) but its inhibition by GS967 (B and C) shortens APD and STV of repolarization (D and E). (A) The TTX-sensitive current density was lower in ventricular cardiomyocytes isolated from CAVB dogs ($n = 4$) than that of SR dogs ($n = 7$). (D) Representative example of action potentials recorded in ventricular cardiomyocytes isolated from CAVB dog at baseline and after exposure to 300 nM GS967 (15 action potentials overlaid for both time points). (E) Relative changes in APD and STV of repolarization induced by GS967 in CAVB cardiomyocytes are respectively represented as white and red bars. The number of cardiomyocytes (isolated from 11 CAVB hearts) recorded (*n*) for each concentration is indicated above corresponding bars. Data are represented as mean ± SD. Unpaired *t*-test: $^{*}P < 0.05$ versus LV SR.

a result, GS967 100, 300 and 1000 nM shortened APD and reduced STV (Figure 2D, E).

GS967 shortens repolarization in sinus rhythm dogs. Intravenous administration of GS967 at 0.03 (low dose) and 0.1 mg·kg^{-1} over 5 min (high dose) yielded peak plasma levels at 5 min (Figure 3A, B). GS967 dose-dependently shortened various repolarization parameters (Figure 3C and Table 1) including QTc from 308 ± 10 to 305 ± 9 ms after low dose and from 307 ± 9 to 297 ± 9 ms after high dose ($P < 0.05$ vs. baseline 2 and vs. low dose; Table 1). While STV remained unchanged by GS967, interventricular dispersion of repolarization (ΔMAPD) was significantly reduced after the high dose (Table 1). Administration of GS967 did not affect heart rate or conduction parameters. GS967 also dose-dependently decreased LV contractility and systolic pressure (Supporting Information Table S1).

GS967 only partly reduces dofetilide-induced afterdepolarizations in vitro

In ventricular cardiomyocytes from SR and CAVB dogs, administration of dofetilide (1 μM) prolonged APD and increased STV before inducing EADs (Figure 4A). Then, superfusion of GS967 (100, 300 and 1000 nM) in the continued presence of dofetilide concentration-dependently reduced the incidence of EADs (Figure 4A, B). At 1000 nM GS967, a concentration that blocks nearly 90% of the late I_{Na} (Figure 2C), EADs remained in 42 and 35% of the cardiomyocytes tested (10/24 and 7/20 cells from SR and CAVB cardiomyocytes, respectively; Figure 4B). Furthermore, the magnitude of the suppression of EADs achieved with GS967 (100 to 1000 nM) was similar in SR and CAVB cardiomyocytes (Figure 4B).

GS967 completely abolishes dofetilide-induced Torsades de Pointes in CAVB dogs despite the remaining presence of ectopic activity

Infusion of dofetilide in the 14 CAVB dogs resulted in the prolongation of all repolarization parameters (QTc and LV MAPD from 400 ± 27 and 266 ± 25 to 624 ± 42 and 477 ± 81 ms, respectively, both $P < 0.05$; Table 2) and increased LV STV (0.9 ± 0.4 to 4.1 ± 2.6 ms, $P < 0.05$) and the interventricular dispersion of repolarization ΔMAPD (from 26 ± 24 to 134 ± 49 ms, $P < 0.05$). Dofetilide induced TdP in 10/14 dogs (Figure 5A, B) and increased the AS (Figure 5C).

The administration of GS967 (0.1 mg·kg^{-1}) completely abolished TdP episodes in all dofetilide-treated dogs

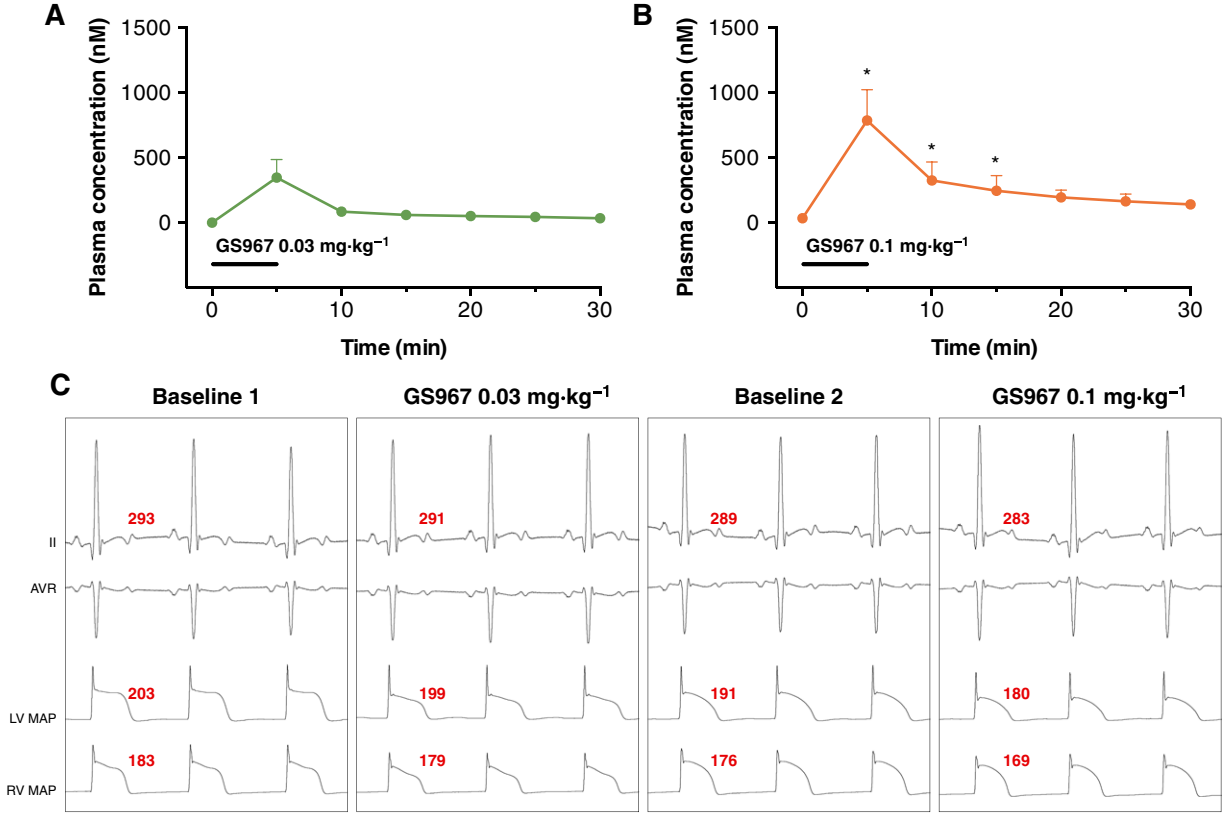

Figure 3

GS967 dose-dependently shortens repolarization in SR dogs. Plasma levels and representative ECG and MAP recordings after administration of GS967 0.03 (A and C) and 0.1 mg·kg^{-1} over 5 min (B and C). For both doses, maximal electrophysiological effects were observed at peak concentrations (5 min) selective for late I_{Na} inhibition. Data are presented as mean ± SD. Paired *t*-test: $^{*}P < 0.05$ versus low dose. QT, LV and RV MAPD are indicated in red on corresponding traces.

Table 1

Electrophysiological effects of GS967 in SR dogs

Parameters (ms)	Baseline 1	GS967 (0.03 mg·kg^{-1})	Baseline 2	GS967 (0.1 mg·kg^{-1})
RR	584 ± 60	588 ± 63	586 ± 58	589 ± 63
PQ	114 ± 15	114 ± 16	118 ± 20	119 ± 20
QRS	76 ± 5	76 ± 6	75 ± 5	75 ± 5
QTc	308 ± 10	305 ± 9	307 ± 9	297 ± 9$^{\#,\dagger}$
LV MAPD	205 ± 9	201 ± 8**	204 ± 12	194 ± 12$^{\#,\dagger}$
RV MAPD	193 ± 8	191 ± 9	189 ± 8	182 ± 8$^{\#,\dagger}$
LV STV	0.3 ± 0.1	0.3 ± 0.1	0.3 ± 0.1	0.3 ± 0.1
RV STV	0.5 ± 0.3	0.4 ± 0.4	0.4 ± 0.2	0.3 ± 0.2
ΔMAPD	12 ± 11	9 ± 11	15 ± 13	11 ± 14$^{\#}$
Plasma level (nM)	–	347 ± 131	–	787 ± 265†

Paired *t*-test:
*$P < 0.05$ versus baseline 1.
$^{\#}P < 0.05$ versus baseline 2.
$^{\dagger}P < 0.05$ versus low dose.

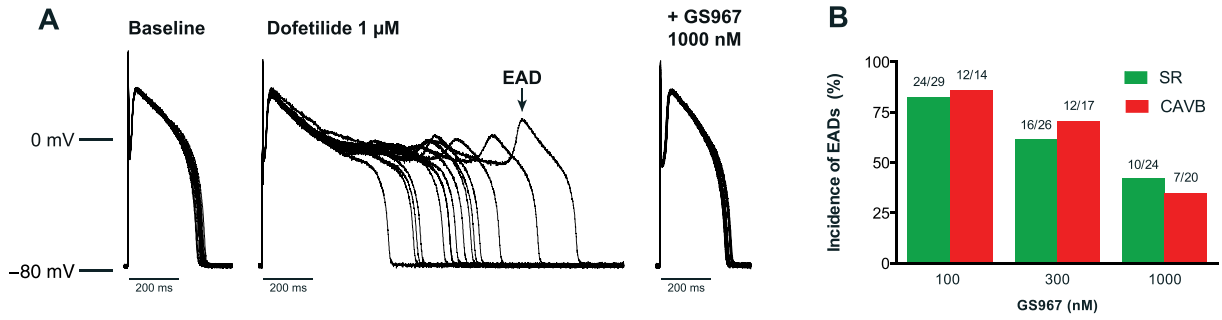

Figure 4

GS967 concentration-dependently reduces dofetilide-induced EADs in ventricular cardiomyocytes. In cells exhibiting reproducible dofetilide (1 µM)-induced EADs, GS967 was superfused at 100, 300 and 1000 nM. (A) Representative example of a successful suppression of dofetilide-induced EADs by 1000 nM GS967 in a ventricular cardiomyocyte isolated from SR dog. (B) Incidence of EADs after GS967 in the continued presence of dofetilide in ventricular cardiomyocytes isolated from 11 SR and 15 CAVB hearts. Data are presented as number of cells with remaining EADs per number of cells with dofetilide-induced EADs.

(Figure 5A, B) and reduced the AS (Figure 5C). While some ectopic activity remained, this strong antiarrhythmic effect was accompanied by a moderate reduction of LV STV (from 4.1 ± 2.6 to 2.5 ± 0.7 ms, *ns*; Table 2) and ΔMAPD (from 134 ± 49 to 86 ± 69 ms, *ns*) as well as a mild, although significant, shortening of QTc (from 624 ± 42 to 561 ± 59 ms, $P < 0.05$; Table 2).

The in vivo antiarrhythmic action of GS967 is associated with reduced spatial intraventricular dispersion of repolarization

The *in vivo* antiarrhythmic effect of GS967 was further investigated in detailed electrical mapping experiments in five CAVB dogs. The administration of dofetilide induced TdP in 3/5 dogs and significantly prolonged repolarization (Table 3). Moreover, the increased severity of the arrhythmic event (dofetilide-induced first EB vs. TdP) was associated with a more pronounced local heterogeneity of repolarization in the LV in all orientations (Table 3). Ectopic activity always arose at the site of maximal heterogeneity (electrode #39 and #74, Figure 6). Infusion of GS967 (0.1 mg·kg^{-1}), as observed in the suppression protocol, completely abolished TdP episodes in the three inducible dogs. This antiarrhythmic effect was associated with a reduction of LV and RV RT and also of LV dispersion of repolarization in the vertical, horizontal and cubic orientations from 167 ± 40, 199 ± 56 and 237 ± 54 ms after dofetilide to 74 ± 31, 82 ± 24 and 123 ± 34 ms after GS967 (all $P < 0.05$; Figure 6 and Table 3).

Discussion

To date, the present study is the first to demonstrate that the selective late I_{Na} inhibitor GS967 completely abolishes drug-induced TdP in CAVB dogs. TdP arrhythmias arise from a

Table 2

Electrophysiological effects of GS967 in suppression of dofetilide-induced TdP arrhythmias in CAVB dogs

	Baseline	Dofetilide	GS967 (0.1 mg·kg^{-1})
Parameters (ms)			
QRS	117 ± 12	118 ± 12	118 ± 12
QTc	400 ± 27	624 ± 42*	561 ± 59$^{\#,*}$
LV MAPD	266 ± 25	477 ± 81*	424 ± 59$^{\#,*}$
RV MAPD	239 ± 22	343 ± 56*	337 ± 31$^{\#,*}$
LV STV	0.9 ± 0.4	4.1 ± 2.6*	2.5 ± 0.7*
RV STV	0.8 ± 0.6	1.7 ± 1.3	1.2 ± 0.3
ΔMAPD	26 ± 24	134 ± 49*	86 ± 69
Arrhythmias			
sEB	2/14	13/14*	9/14*
mEB	0/14	12/14*	2/14$^{\#}$
TdP	0/14	10/14*	0/14$^{\#}$
AS	1.1 ± 0.4	28.1 ± 27.9*	2.0 ± 1.1$^{\#}$

Parametric (electrophysiological parameters) and non-parametric (AS) repeated measurement ANOVA McNemar test (arrhythmia incidence).

*$P < 0.05$ versus baseline.

$^{\#}P < 0.05$ versus dofetilide.

multifactorial process involving action potential prolongation and the associated occurrence of afterdepolarizations initiating events and an increase in intraventricular spatial dispersion of repolarization for arrhythmia perpetuation. In the current study, the use of *in vitro* assays using canine ventricular cardiomyocytes allowed us to study in detail the initiating mechanism of the arrhythmia, while the *in vivo* assay provided the next level of complexity by adding the component of spatial dispersion (Dunnink *et al.*, 2017). In general, we observed a statistically significant but modest effect of GS967 on the initiating events of TdP arrhythmia, as seen by a 60–65% reduction on EADs *in vitro* and the remaining presence of sEB *in vivo* in 65% of CAVB dogs. In comparison, we found a robust and statistically significant, but yet not complete, reversal of spatial dispersion of repolarization *in vivo* upon GS967 application in hearts challenged with dofetilide. Our data suggest that the antiarrhythmic action of GS967 is predominantly based on reduction of spatial dispersion. However, its mode of action seems to rather lie on the prevention of arrhythmia perpetuation than the suppression of the initiating trigger.

Selective late I_{Na} inhibition shortens repolarization

GS967 is a highly selective late I_{Na} inhibitor, with minimal effects on the peak I_{Na} and I_{Kr} that are responsible for the additional effects of flecainide and ranolazine, which respectively slows conduction and prolongs repolarization (Belardinelli *et al.*, 2013). In the present study, GS967 strongly shortened APD of ventricular cardiomyocytes in accordance with the concentration-dependent inhibition of the late I_{Na} (100–1000 nM) and stabilized the repolarization process as reflected by the significant reduction in STV.

Likewise, GS967 significantly shortened QTc of SR dogs at plasma levels selective for late I_{Na} inhibition, while AV (PQ interval) and ventricular (QRS interval) conduction was not affected. No reduction of STV was observed because these dogs with unremodelled ventricles still possess a normal repolarization reserve.

Our data support the previous findings obtained in rabbit-isolated ventricular myocytes (Belardinelli *et al.*, 2013), canine Purkinje fibres (Sicouri *et al.*, 2013), Langendorff-perfused rabbit heart (Belardinelli *et al.*, 2013) and anaesthetized rabbits (Belardinelli *et al.*, 2013), which all reported a concentration- and dose-dependent shortening of repolarization resulting from the late I_{Na} inhibition by GS967.

Moderate reduction of early afterdepolarizations in canine ventricular cardiomyocytes

Despite the significant and marked reduction of APD and STV, GS967 only mildly suppressed dofetilide-induced EADs in canine ventricular cardiomyocytes. Based on its IC_{50} for late I_{Na} determined in these myocytes (about 200 nM), the range of concentrations tested is selective for the late I_{Na} inhibition. However, at the highest concentration (1000 nM), which blocked nearly 90% of late I_{Na}, EADs remained present in 35–40% of the cells. Our findings contrast with previous studies that reported the strong suppression by GS967 (300 nM) of EADs induced either by the late I_{Na} enhancer **ATX-II** or the I_{Kr} blocker **E-4031** in rabbit ventricular cardiomyocytes (Belardinelli *et al.*, 2013) or in canine Purkinje fibres (Sicouri *et al.*, 2013) as well as delayed afterdepolarizations induced by **isoprenaline** and/or calcium in canine Purkinje fibres (Sicouri *et al.*, 2013). The differences in antiarrhythmic effect may be explained by the interspecies difference and the shorter basic cycle length used in rabbit myocytes (1 Hz) compared with our ventricular dog cardiomyocytes (0.5 Hz), potentially leading to a reduced APD prolongation and EAD incidence upon the reverse use-dependent I_{Kr} block by dofetilide or E-4031. Isolated canine cardiomyocytes are very sensitive for developing EADs upon a 'single hit' on their repolarization process (Nalos *et al.*, 2012). Therefore, the persistence of EADs in ventricular cardiomyocytes following antiarrhythmic interventions requires further *in vivo* confirmation as exemplified in this study.

In our hands, the selective late I_{Na} inhibition by GS967 does not seem to restore calcium handling to ensure a proper repolarization process in isolated ventricular cardiomyocytes. Therefore, follow-up experiments would be required to assess in detail the effect of GS967 on cytosolic sodium and calcium concentrations.

Remarkably, GS967 similarly suppressed EADs in SR as in CAVB cardiomyocytes. Although this study confirms the reduction of late I_{Na} density in CAVB conditions (Antoons *et al.*, 2010), the potency of GS967 to block the late I_{Na} is similar in SR and CAVB cells (IC_{50} 188 ± 15 and 230 ± 10 nM, respectively). Therefore, it would suggest that the magnitude of late I_{Na} density does not play a critical role

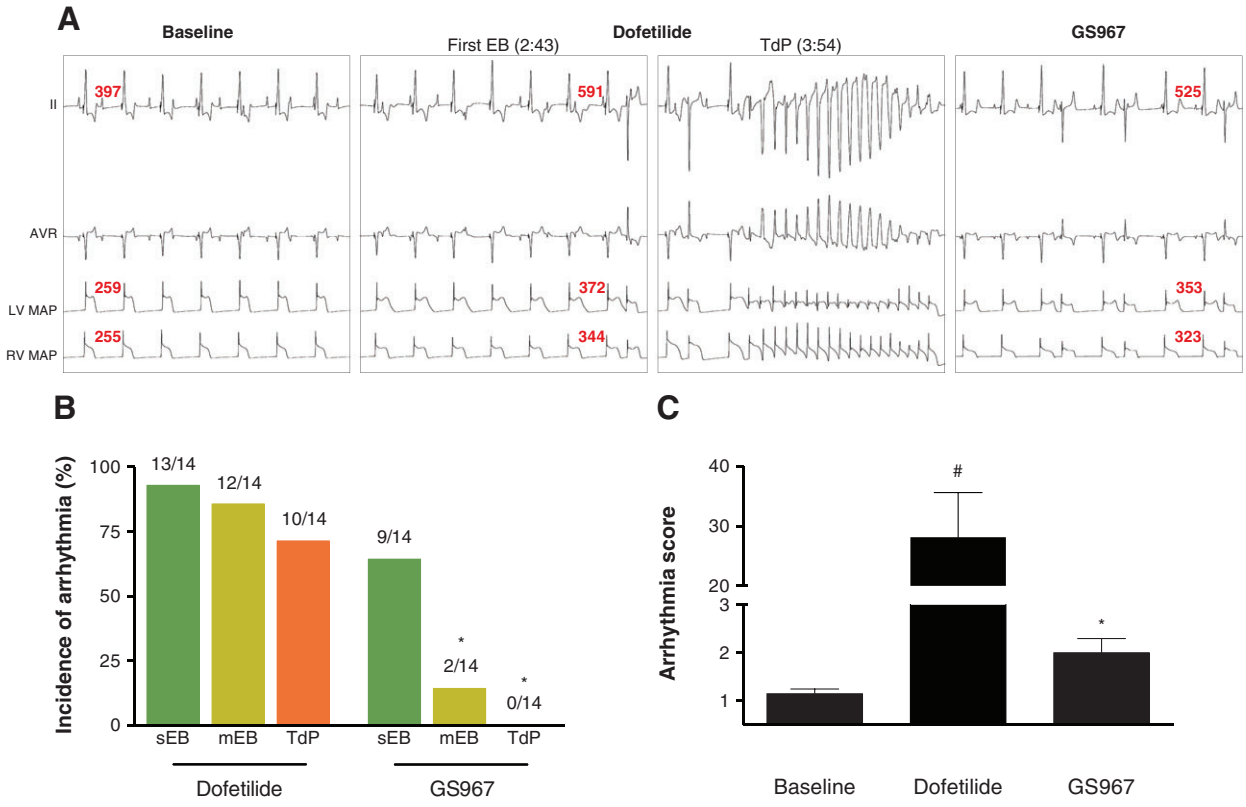

Figure 5

GS967 completely abolishes dofetilide-induced TdP arrhythmias in CAVB dogs. (A) Representative ECG, LV and RV MAP traces are depicted for baseline, before the first EB and TdP induced by dofetilide and after GS967 0.1 mg·kg^{-1} administration. (B) Incidence of arrhythmic events (sEB, mEB and TdP) after dofetilide and GS967 treatments. Data are presented as number of dogs with events per number of dogs tested. (C) AS, a surrogate parameter for arrhythmia severity, is presented as mean ± SEM. McNemar test (incidence of arrhythmia) and non-parametric repeated measurement ANOVA (AS): $^{\#}P < 0.05$ versus baseline; $^{*}P < 0.05$ versus dofetilide. QT, LV and RV MAPD are indicated as red numbers.

in the moderate *in vitro* antiarrhythmic effect of GS967, a finding also observed with TTX, which exerted a similar suppressive effect in SR and CAVB cardiomyocytes (Antoons *et al.*, 2010).

Dofetilide-induced TdP is suppressed by GS967 in CAVB dogs

Despite the reduced late I_{Na} density in CAVB conditions, the mild antiarrhythmic effect against EADs *in vitro* and incomplete inhibition of ectopy *in vivo*, GS967 completely suppressed dofetilide-induced TdP in CAVB dogs. This effect was not associated with either a strong reduction in repolarization or in STV, most likely due to the remaining ectopic activity in most animals. Previous *ex vivo* studies performed in Langendorff-perfused hearts from rat and rabbit demonstrated a similar antiarrhythmic effect of GS967 against ATX-II, E-4031 (Belardinelli *et al.*, 2013), **aconitine**- (Pezhouman *et al.*, 2014) and hypokalaemia-induced (Pezhouman *et al.*, 2015) ventricular arrhythmias. Likewise *in vivo*, GS967 exerted a strong antiarrhythmic effect in terminating or shortening ventricular tachycardia episodes in methoxamine-sensitized and ischaemic rabbits (Belardinelli *et al.*, 2013) as well as in pig models of ischaemia- (Bonatti *et al.*, 2014) and catecholamine-induced (Alves Bento *et al.*, 2015) arrhythmias.

Arrhythmia perpetuation is curtailed by GS967 via the reduction of spatial dispersion of repolarization

In this study, the inhibition of late I_{Na} induced by GS967 completely suppressed dofetilide-induced TdP in CAVB dogs, while some ectopic activity remained in the majority (65%) of animals. The detailed mapping experiments demonstrated that this antiarrhythmic effect was associated with a partial, but significant, reversal of intraventricular spatial dispersion of repolarization. Similarly, several studies previously documented the reduction by GS967 of the 2D spatial dispersion in Langendorff-perfused rat hearts (Pezhouman *et al.*, 2014), T-wave alternans in pig models of catecholamine (Alves Bento *et al.*, 2015) and ischaemia-induced (Bonatti *et al.*, 2014) ventricular tachycardia. The antiarrhythmic efficacy of a number of drugs, including the late I_{Na} blockers ranolazine and vernakalant, has been associated with a reduction of the spatial dispersion of repolarization (Milberg *et al.*, 2005; 2008; 2011; Sossalla *et al.*, 2014; Frommeyer *et al.*, 2017), but only in Langendorff-perfused intact heart or

Table 3

Effect of GS967 on spatial dispersion of repolarization after dofetilide-induced TdP arrhythmias in CAVB dogs

Parameters (ms)	Baseline	Dofetilide (first EB)	Dofetilide (TdP/5 min)	GS967 (0.1 mg·kg^{-1})
Repolarization				
LV RT	320 ± 26	425 ± 54*	484 ± 48*	402 ± 43$^{\#,*}$
RV RT	277 ± 22	351 ± 57	383 ± 35*	355 ± 38$^{\#,*}$
ΔRT	43 ± 13	74 ± 24	101 ± 45	47 ± 15
LS RT	322 ± 23	430 ± 52	493 ± 66	409 ± 46
RS RT	313 ± 22	404 ± 28	468 ± 61	387 ± 30
LV dispersion (n = 5)				
Transmural	51 ± 4	139 ± 58	169 ± 60*	97 ± 29
Vertical	46 ± 11	119 ± 39	167 ± 40*	74 ± 31$^{\#}$
Horizontal	57 ± 14	145 ± 49	199 ± 56*	82 ± 24$^{\#}$
Cubic	68 ± 14	203 ± 54*	237 ± 54*	123 ± 34$^{\#}$
Septum dispersion (n = 3)				
Transmural	34 ± 6	127 ± 65	147 ± 31	75 ± 28
Vertical	39 ± 9	145 ± 43	173 ± 29	86 ± 23
Horizontal	24 ± 5	105 ± 80	105 ± 62	49 ± 30
Cubic	47 ± 5	177 ± 62	198 ± 19	94 ± 14

ΔRT, interventricular dispersion of repolarization determined as LV RT - RV RT; LS, left side of septal wall; RS, right side of septal wall.
Repeated measurement ANOVA:
*$P < 0.05$ versus baseline.
$^{\#}P < 0.05$ versus dofetilide (TdP).

wedge preparations in which the input from mechanical workload or the autonomic nervous system is absent. Our study is the first to investigate the antiarrhythmic effect of GS967 associated with the reduction of spatial dispersion of repolarization in an intact animal. In the CAVB dog model, all detailed mapping studies emphasize the importance of focal origin, resulting from a triggered activity mechanism, in the initiation of an arrhythmic episode (Kozhevnikov *et al.*, 2002; Schreiner *et al.*, 2004; Boulaksil *et al.*, 2011; Dunnink *et al.*, 2017). Recently, our group demonstrated that the local heterogeneity of repolarization was significantly higher before a TdP than prior to the first sEB, indicating the close correlation between the magnitude of spatial dispersion of repolarization and the severity of the following arrhythmic event (Dunnink *et al.*, 2017). Based on *in vitro* and *in vivo* findings, GS967 does not suppress significantly the initiation of an arrhythmic event, as seen with the remaining EADs in myocytes and ectopic activity in the majority of CAVB dogs. Nevertheless, GS967 administration significantly reduced intraventricular spatial dispersion of repolarization in all orientations (transmural, horizontal, vertical and cubic) to such an extent that the perpetuation of an arrhythmic episode could not be maintained.

In the five CAVB dogs undergoing electrical mapping experiments, endocardial and subendocardial regions exhibited greater RT increase upon dofetilide administration. After infusion of GS967, the magnitude of RT shortening was also higher in these regions. Although the late I_{Na} density was reduced in CAVB cardiomyocytes, the transmural gradient of late I_{Na}, which could represent an important contributor, remains to be explored. Nevertheless, our *in vitro* experiments show that under conditions of I_{Kr} blockade, prolongation of repolarization is largely associated with a longer plateau phase (Figure 4A). During this phase, the membrane resistance is high and a small change in currents, depolarizing or repolarizing, can cause a large shift in voltage and considerably affect the duration of the action potential. In addition, at these membrane potentials, sodium channels may remain activated or recover from inactivation, resulting in a sustained late I_{Na}. Therefore, it may explain that, upon selective late I_{Na} inhibition by GS967, the magnitude of repolarization shortening is greater within regions of longer RT than those with shorter ones, contributing to the reduction of spatial dispersion of repolarization.

Additionally, in three out of five CAVB dogs undergoing cardiac electrical mapping, the activation delay (time between the first and last activated electrode) of the remaining sEB still occurring after GS967 administration was shorter than that of the first EB of a TdP episode previously induced by dofetilide in the same dog (33.5 ± 2.2 vs. 64.9 ± 34.9 ms, respectively). It is well known that the spatial dispersion of repolarization plays a critical role in the generation of functional block, necessary for ectopic activity to take place (Restivo *et al.*, 2004). Under conditions of reduced spatial dispersion of repolarization, as observed after GS967 administration, the overall ventricular activation during the EBs is more synchronous as a result of homogenous cardiac refractoriness.

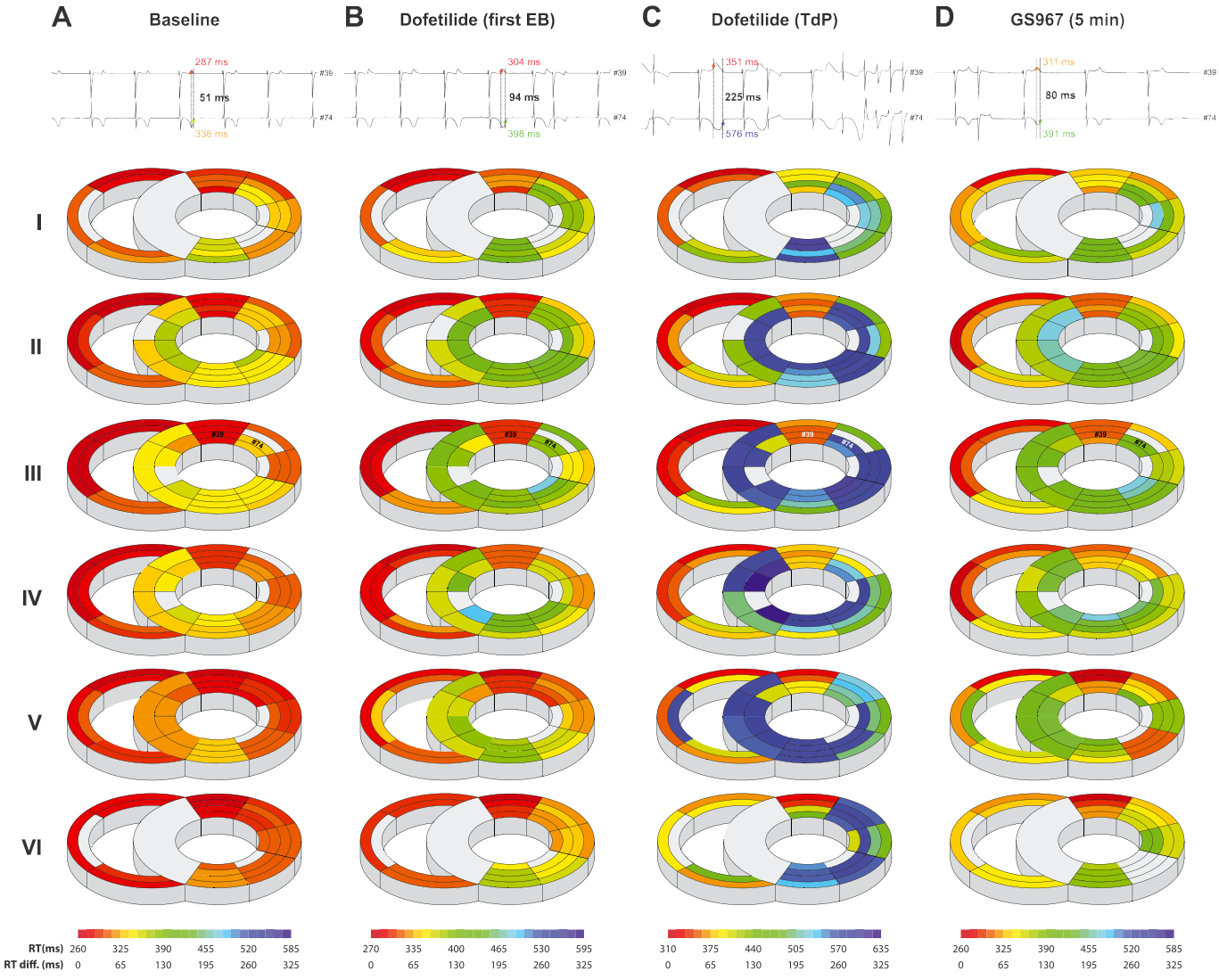

Figure 6

The reduction of spatial dispersion of repolarization underlies the *in vivo* antiarrhythmic effect of GS967 (0.1 mg·kg^{-1}) in CAVB dogs. Representative example of the repolarization pattern in the LV, RV and septal wall at the different levels of the heart (from base I to apex VI) at baseline (A), before dofetilide-induced first EB (B) and TdP (C) and following GS967 (0.1 mg·kg^{-1}) administration (D) in a CAVB dog undergoing electrical mapping experiment. For each period, traces (with end of RT symbolized by a coloured dot and corresponding time) depict unipolar electrograms (EGMs) from the region surrounding the origin of arrhythmia, where the highest dispersion of repolarization was observed upon dofetilide administration. The suppression of TdP by GS967 was accompanied by a significant reduction of local spatial dispersion of repolarization (D). Grey regions represent low EGM amplitudes discarded from the analysis. RT, repolarization time (absolute values relative to stimulus artefact); RT diff., difference in repolarization time (relative to the first repolarized region).

A different mode of action of GS967 compared with other highly efficient antiarrhythmic drugs

In the CAVB dog model, the very strong antiarrhythmic effect of GS967 against TdP [complete (100%) suppression of TdP] resembled that of the I_{CaL} blockers flunarizine and **verapamil** (Oros *et al.*, 2010) and the Na–Ca exchanger inhibitor **SEA0400** (Bourgonje *et al.*, 2013). However, unlike GS967, all these drugs restored STV to baseline levels and significantly diminished ectopic activity (Bossu *et al.*, 2017). Unfortunately, in comparison with GS967 as shown in this study, detailed mapping studies on the effect of flunarizine, verapamil and SEA0400 on intraventricular spatial dispersion of repolarization in the CAVB dog are lacking to date. Therefore, we cannot exclude the possibility that these compounds, in addition to preventing ectopy and EADs, will also reduce intraventricular spatial dispersion of repolarization in CAVB dogs in a similar fashion to that observed in other *ex vivo* models (Milberg *et al.*, 2005; Milberg *et al.*, 2008). Nevertheless, the *in vitro* data on suppression of dofetilide-induced EADs demonstrate that, unlike GS967, flunarizine (Oros *et al.*, 2010) and SEA0400 (Bourgonje *et al.*, 2013) are able to completely suppress EADs in isolated cells,

pointing to an *in vivo* antiarrhythmic action primarily based on suppressing the initiating trigger (afterdepolarizations).

Conclusion

In this study, selective late I_{Na} inhibition by GS967 shortened repolarization *in vitro* and *in vivo*. Despite the mild reduction of EADs in canine ventricular cardiomyocytes and a lower late I_{Na} density in CAVB conditions, GS967 exerted a robust antiarrhythmic effect *in vivo* by terminating all dofetilide-induced TdP. This effect was associated with a marked reduction of intraventricular spatial dispersion of repolarization. Together, our data suggest that GS967 does not interfere in a major way with the initiating trigger of arrhythmia while the actual perpetuation of arrhythmic episodes is prevented and associated with a reduced intraventricular spatial heterogeneity of repolarization.

Acknowledgement

This work was supported by Gilead Sciences, Inc.

Author contributions

A.B., M.J.C.H., V.M.F.M., R.V., H.D.M.B., A.D., J.M.T.D.B. and N.M. planned and performed the experiments. A.B., M.J.C.H., H.D.M.B., A.D., N.M., M.A.G.V.D.H. and M.A.V. analysed the data. A.B., S.R., L.B., M.A.G.V.D.H. and M.A.V. designed the study and wrote the manuscript.

Conflict of interest

N.M., S.R. and L.B. are former employees of Gilead Sciences, Inc.

Declaration of transparency and scientific rigour

This Declaration acknowledges that this paper adheres to the principles for transparent reporting and scientific rigour of preclinical research recommended by funding agencies, publishers and other organisations engaged with supporting research.

References

Alexander SPH, Striessnig J, Kelly E, Marrion NV, Peters JA, Faccenda E *et al*. (2017). The Concise Guide to PHARMACOLOGY 2017/18: Voltage-gated ion channels. Br J Pharmacol 174: S160–S194.

Allen LA, Stevenson LW, Grady KL, Goldstein NE, Matlock DD, Arnold RM *et al*. (2012). Decision making in advanced heart failure: a scientific statement from the American Heart Association. Circulation 125: 1928–1952.

Allen TJ, Chapman RA (1996). Effects of ranolazine on L-type calcium channel currents in guinea-pig single ventricular myocytes. Br J Pharmacol 118: 249–254.

Alves Bento AS, Bacic D, Saran Carneiro J, Nearing BD, Fuller H, Justo FA *et al*. (2015). Selective late I_{Na} inhibition by GS967 exerts parallel suppression of catecholamine-induced hemodynamically significant ventricular tachycardia and T-wave alternans in an intact porcine model. Heart Rhythm 12: 2508–2514.

Antoons G, Oros A, Beekman JD, Engelen MA, Houtman MJ, Belardinelli L *et al*. (2010). Late Na^+ current inhibition by ranolazine reduces torsades de pointes in the chronic atrioventricular block dog model. J Am Coll Cardiol 55: 801–809.

Antzelevitch C, Belardinelli L, Zygmunt AC, Burashnikov A, Di Diego JM, Fish JM *et al*. (2004). Electrophysiological effects of ranolazine, a novel antianginal agent with antiarrhythmic properties. Circulation 110: 904–910.

Antzelevitch C, Nesterenko V, Shryock JC, Rajamani S, Song Y, Belardinelli L (2014). The role of late I_{Na} in development of cardiac arrhythmias. Handb Exp Pharmacol 221: 137–168.

Belardinelli L, Giles WR, Rajamani S, Karagueuzian HS, Shryock JC (2015). Cardiac late Na_+ current: proarrhythmic effects, roles in long QT syndromes, and pathological relationship to CaMKII and oxidative stress. Heart Rhythm 12: 440–448.

Belardinelli L, Liu G, Smith-Maxwell C, Wang WQ, El-Bizri N, Hirakawa R *et al*. (2013). A novel, potent, and selective inhibitor of cardiac late sodium current suppresses experimental arrhythmias. J Pharmacol Exp Ther 344: 23–32.

Bezzina CR, Lahrouchi N, Priori SG (2015). Genetics of sudden cardiac death. Circ Res 116: 1919–1936.

Bonatti R, Silva AF, Batatinha JA, Sobrado LF, Machado AD, Varone BB *et al*. (2014). Selective late sodium current blockade with GS967 markedly reduces ischemia-induced atrial and ventricular repolarization alternans and ECG heterogeneity. Heart Rhythm 11: 1827–1835.

Bossu A, Varkevisser R, Beekman HDM, Houtman MJC, van der Heyden MAG, Vos MA (2017). Short-term variability of repolarization is superior to other repolarization parameters in the evaluation of diverse antiarrhythmic interventions in the chronic atrioventricular block dog. J Cardiovasc Pharmacol 69: 398–407.

Boulaksil M, Jungschleger JG, Antoons G, Houtman MJ, de Boer TP, Wilders R *et al*. (2011). Drug-induced torsade de pointes arrhythmias in the chronic AV block dog are perpetuated by focal activity. Circ Arrhythm Electrophysiol 4: 566–576.

Bourgonje VJ, Vos MA, Ozdemir S, Doisne N, Acsai K, Varro A *et al*. (2013). Combined Na^+/Ca^{2+} exchanger and L-type calcium channel block as a potential strategy to suppress arrhythmias and maintain ventricular function. Circ Arrhythm Electrophysiol 6: 371–379.

Burashnikov A, Di Diego JM, Goodrow RJ Jr, Belardinelli L, Antzelevitch C (2015). Atria are more sensitive than ventricles to GS967-induced inhibition of late sodium current. J Cardiovasc Pharmacol Ther 20: 501–508.

Carneiro JS, Bento AS, Bacic D, Nearing BD, Rajamani S, Belardinelli L *et al*. (2015). The selective cardiac late sodium current inhibitor GS967 suppresses autonomically triggered atrial fibrillation in an intact porcine model. J Cardiovasc Electrophysiol 26: 1364–1369.

Chaitman BR, Skettino SL, Parker JO, Hanley P, Meluzin J, Kuch J *et al*. (2004). Anti-ischemic effects and long-term survival during ranolazine monotherapy in patients with chronic severe angina. J Am Coll Cardiol 43: 1375–1382.

Curtis MJ, Bond RA, Spina D, Ahluwalia A, Alexander SP, Giembycz MA *et al*. (2015). Experimental design and analysis and their reporting: new guidance for publication in BJP. Br J Pharmacol 172: 3461–3471.

Dunnink A, Stams TRG, Bossu A, Meijborg VMF, Beekman JDM, Wijers SC *et al*. (2017). Torsade de pointes arrhythmias arise at the site of maximal heterogeneity of repolarization in the chronic complete atrioventricular block dog. Europace 19: 858–865.

Fernandes S, Hoyer K, Liu G, Wang WQ, Dhalla AK, Belardinelli L *et al*. (2014). Selective inhibition of the late sodium current has no adverse effect on electrophysiological or contractile function of the normal heart. J Cardiovasc Pharmacol 63: 512–519.

Frommeyer G, Clauss C, Ellermann C, Bogossian H, Dechering DG, Kochhauser S *et al*. (2017). Antiarrhythmic effect of vernakalant in an experimental model of long-QT-syndrome. Europace 19: 866–873.

Harding SD, Sharman JL, Faccenda E, Southan C, Pawson AJ, Ireland S *et al*. (2018). The IUPHAR/BPS Guide to PHARMACOLOGY in 2018: updates and expansion to encompass the new guide to IMMUNOPHARMACOLOGY. Nucl Acids Res 46: D1091–D1106.

Kilkenny C, Browne W, Cuthill IC, Emerson M, Altman DG, Group NCRRGW (2010). Animal research: reporting *in vivo* experiments: the ARRIVE guidelines. Br J Pharmacol 160: 1577–1579.

Kozhevnikov DO, Yamamoto K, Robotis D, Restivo M, El-Sherif N (2002). Electrophysiological mechanism of enhanced susceptibility of hypertrophied heart to acquired torsade de pointes arrhythmias: tridimensional mapping of activation and recovery patterns. Circulation 105: 1128–1134.

Maltsev VA, Undrovinas AI (2006). A multi-modal composition of the late Na^+ current in human ventricular cardiomyocytes. Cardiovasc Res 69: 116–127.

McGrath JC, Lilley E (2015). Implementing guidelines on reporting research using animals (ARRIVE etc.): new requirements for publication in BJP. Br J Pharmacol 172: 3189–3193.

Milberg P, Frommeyer G, Kleideiter A, Fischer A, Osada N, Breithardt G *et al*. (2011). Antiarrhythmic effects of free polyunsaturated fatty acids in an experimental model of LQT2 and LQT3 due to suppression of early afterdepolarizations and reduction of spatial and temporal dispersion of repolarization. Heart Rhythm 8: 1492–1500.

Milberg P, Pott C, Fink M, Frommeyer G, Matsuda T, Baba A *et al*. (2008). Inhibition of the Na^+/Ca^{2+} exchanger suppresses torsades de pointes in an intact heart model of long QT syndrome-2 and long QT syndrome-3. Heart Rhythm 5: 1444–1452.

Milberg P, Reinsch N, Osada N, Wasmer K, Monnig G, Stypmann J *et al*. (2005). Verapamil prevents torsade de pointes by reduction of transmural dispersion of repolarization and suppression of early afterdepolarizations in an intact heart model of LQT3. Basic Res Cardiol 100: 365–371.

Nalos L, Varkevisser R, Jonsson MK, Houtman MJ, Beekman JD, van der Nagel R *et al*. (2012). Comparison of the I_{Kr} blockers moxifloxacin, dofetilide and E-4031 in five screening models of pro-arrhythmia reveals lack of specificity of isolated cardiomyocytes. Br J Pharmacol 165: 467–478.

Oros A, Beekman JD, Vos MA (2008). The canine model with chronic, complete atrio-ventricular block. Pharmacol Ther 119: 168–178.

Oros A, Houtman MJ, Neco P, Gomez AM, Rajamani S, Oosterhoff P *et al*. (2010). Robust anti-arrhythmic efficacy of verapamil and flunarizine against dofetilide-induced TdP arrhythmias is based upon a shared and a different mode of action. Br J Pharmacol 161: 162–175.

Parikh A, Mantravadi R, Kozhevnikov D, Roche MA, Ye Y, Owen LJ *et al*. (2012). Ranolazine stabilizes cardiac ryanodine receptors: a novel mechanism for the suppression of early afterdepolarization and torsades de pointes in long QT type 2. Heart Rhythm 9: 953–960.

Pezhouman A, Madahian S, Stepanyan H, Ghukasyan H, Qu Z, Belardinelli L *et al*. (2014). Selective inhibition of late sodium current suppresses ventricular tachycardia and fibrillation in intact rat hearts. Heart Rhythm 11: 492–501.

Pezhouman A, Singh N, Song Z, Nivala M, Eskandari A, Cao H *et al*. (2015). Molecular basis of hypokalemia-induced ventricular fibrillation. Circulation 132: 1528–1537.

Pulford BR, Kluger J (2016). Ranolazine therapy in cardiac arrhythmias. Pacing Clin Electrophysiol: PACE 39: 1006–1015.

Restivo M, Caref EB, Kozhevnikov DO, El-Sherif N (2004). Spatial dispersion of repolarization is a key factor in the arrhythmogenicity of long QT syndrome. J Cardiovasc Electrophysiol 15: 323–331.

Saint DA (2008). The cardiac persistent sodium current: an appealing therapeutic target? Br J Pharmacol 153: 1133–1142.

Schram G, Zhang L, Derakhchan K, Ehrlich JR, Belardinelli L, Nattel S (2004). Ranolazine: ion-channel-blocking actions and *in vivo* electrophysiological effects. Br J Pharmacol 142: 1300–1308.

Schreiner KD, Voss F, Senges JC, Becker R, Kraft P, Bauer A *et al*. (2004). Tridimensional activation patterns of acquired torsade-de-pointes tachycardias in dogs with chronic AV-block. Basic Res Cardiol 99: 288–298.

Shryock JC, Song Y, Rajamani S, Antzelevitch C, Belardinelli L (2013). The arrhythmogenic consequences of increasing late I_{Na} in the cardiomyocyte. Cardiovasc Res 99: 600–611.

Sicouri S, Belardinelli L, Antzelevitch C (2013). Antiarrhythmic effects of the highly selective late sodium channel current blocker GS967. Heart Rhythm 10: 1036–1043.

Sipido KR, Volders PG, Schoenmakers M, De Groot SH, Verdonck F, Vos MA (2002). Role of the Na/Ca exchanger in arrhythmias in compensated hypertrophy. Ann N Y Acad Sci 976: 438–445.

Sossalla S, Wallisch N, Toischer K, Sohns C, Vollmann D, Seegers J *et al*. (2014). Effects of ranolazine on torsades de pointes tachycardias in a healthy isolated rabbit heart model. Cardiovasc Ther 32: 170–177.

Tamargo J, Capucci A, Mabo P (2012). Safety of flecainide. Drug Saf 35: 273–289.

Thomsen MB, Verduyn SC, Stengl M, Beekman JD, de Pater G, van Opstal J *et al*. (2004). Increased short-term variability of repolarization predicts d-sotalol-induced torsades de pointes in dogs. Circulation 110: 2453–2459.

Zaza A, Belardinelli L, Shryock JC (2008). Pathophysiology and pharmacology of the cardiac "late sodium current". Pharmacol Ther 119: 326–339.

Supporting Information

Additional Supporting Information may be found online in the supporting information tab for this article.

https://doi.org/10.1111/bph.14217

Table S1 Hemodynamic effects of GS967 in sinus rhythm dogs.

Data S1 Identification of dogs for animal and cellular experiments.